DETAILS OF BLAST INTERACTION WITH STRUCTURES

Louk H.J. Absil, H.H. (Boy) Kodde, W. Paul M. Mercx and Rolf M.M. van Wees

TNO Prins Maurits Laboratory
P.O. Box 45
2280 AA Rijswijk
The Netherlands
tel. +31.15.842842
fax. +31.15.843991

Abstract

The paper addresses details of blast interaction with structures. It is based on three test programmes performed in recent years at TNO Prins Maurits Laboratory. These programmes were:

o   Effectiveness of blastwalls. This programme was aimed at optimising the reduction in blast strength from large calibre weapon firings that can be gained with blastwalls.

o   Shock Interaction with Multiple Obstacles. This programme is aimed at understanding the reduction in shock strength as it passes obstacles, in particular when a blast wave enters a buildup area. Numerical simulations were made, which were validated and complemented by experiments in a shock tube.

o   Entering of shock in a building. This programme was aimed at understanding the internal load on a building caused by a blast wave when it enters through a broken window. Experiments were performed with a chamber placed in front of our 2 m diameter blast simulator.

Although all the fundamentals of shock interaction with structures are known, practical situations produce such a complicated pattern of reflections and rarefactions that prediction of the interaction becomes difficult. This paper focuses on the details of the interaction process and on the overall results of the programmes.

1. REPORT DATE	2. REPORT TYPE	3. DATES COVERED
AUG 1994		**00-00-1994 to 00-00-1994**

4. TITLE AND SUBTITLE	5a. CONTRACT NUMBER
Details of Blast Interaction with Structures	5b. GRANT NUMBER
	5c. PROGRAM ELEMENT NUMBER
6. AUTHOR(S)	5d. PROJECT NUMBER
	5e. TASK NUMBER
	5f. WORK UNIT NUMBER
7. PERFORMING ORGANIZATION NAME(S) AND ADDRESS(ES)	8. PERFORMING ORGANIZATION REPORT NUMBER
TNO Prins Maurits Laboratory,P.O. Box 45,2280 AA Rijswijk,The Netherlands,	
9. SPONSORING/MONITORING AGENCY NAME(S) AND ADDRESS(ES)	10. SPONSOR/MONITOR'S ACRONYM(S)
	11. SPONSOR/MONITOR'S REPORT NUMBER(S)

12. DISTRIBUTION/AVAILABILITY STATEMENT
Approved for public release; distribution unlimited

13. SUPPLEMENTARY NOTES
See also ADM000767. Proceedings of the Twenty-Sixth DoD Explosives Safety Seminar Held in Miami, FL on 16-18 August 1994.

14. ABSTRACT
see report

15. SUBJECT TERMS

16. SECURITY CLASSIFICATION OF:			17. LIMITATION OF ABSTRACT	18. NUMBER OF PAGES	19a. NAME OF RESPONSIBLE PERSON
a. REPORT	b. ABSTRACT	c. THIS PAGE	**Same as Report (SAR)**	**22**	
unclassified	**unclassified**	**unclassified**			

Keywords

Blast waves, Blast loads, Blast measurement, Diffraction, Shock waves

1   Introduction

Despite the fact that all the fundamentals of shock interaction with structures are known, diffraction of shock waves with practical structures produce generally such complicated patterns of reflection waves and rarefaction waves that prediction of the interaction becomes difficult. In addition, shock waves display non-linear behaviour, so the most simple prediction method, based on linear acoustic theory, does not give accurate predictions in many cases. Scale model tests or numerical simulation with Computational Fluid Dynamics codes are then the only options. The alternative, of course, is to check in the literature whether a similar problem to your own has already been solved by someone else.

This paper presents some selected results of three research programmes on the interaction of weak shock waves with structures that were carried out in recent years at TNO Prins Maurits Laboratory. These programmes were:

o   Effectiveness of blastwalls. This programme was aimed at optimising the reduction in blast strength from large calibre weapon firings that can be gained with blastwalls.

o   Shock Interaction with Multiple Obstacles. This programme is aimed at understanding the reduction in shock strength as it passes obstacles, in particular when a blast wave enters a buildup area. Numerical simulations were made, which were validated and complemented by experiments in a shock tube.

o   Entering of shock in a building. This programme was aimed at understanding the internal load on a building caused by a blast wave when it enters through a broken window. Experiments were performed with a chamber placed in front of our 2 m diameter blast simulator.

The paper focuses on the details of the interaction process and on the overall results of the programmes. More information about the programmes, in particular on the experimental set-up, can be found in the references.

2   Diffraction of a shock wave over a single wall

2.1   Purpose

In a densely populated country like the Netherlands noise pollution from artillery or large-calibre training facilities poses a severe problem to neighbouring communities. One way to attenuate the blast in the far field is the construction of blast walls close to the gun. Since part of the shock wave will be reflected by the barrier, the blast behind it will be attenuated and the noise reduced. Although much information is available on the reduction of sound by screens,

very little exists on the reduction of blast. Therefore an experimental and theoretical programme was carried out to investigate the blast reduction by blast walls. As part of this programme the diffraction of shock waves over the blast wall was studied.

2.2   Investigation method

One part of the programme used scale model tests. To this end, a 1:10 scale model of a howitzer training site was built at TNO-PML. Figure l shows a sketch of the experimental set-up.

Figure 1 Experimental set-up 1:10 scale model tests. The points labelled P1 to P8 are pressure transducer locations; d_s and h_s indicate the location of the source (detonator). All dimensions are given in metres.
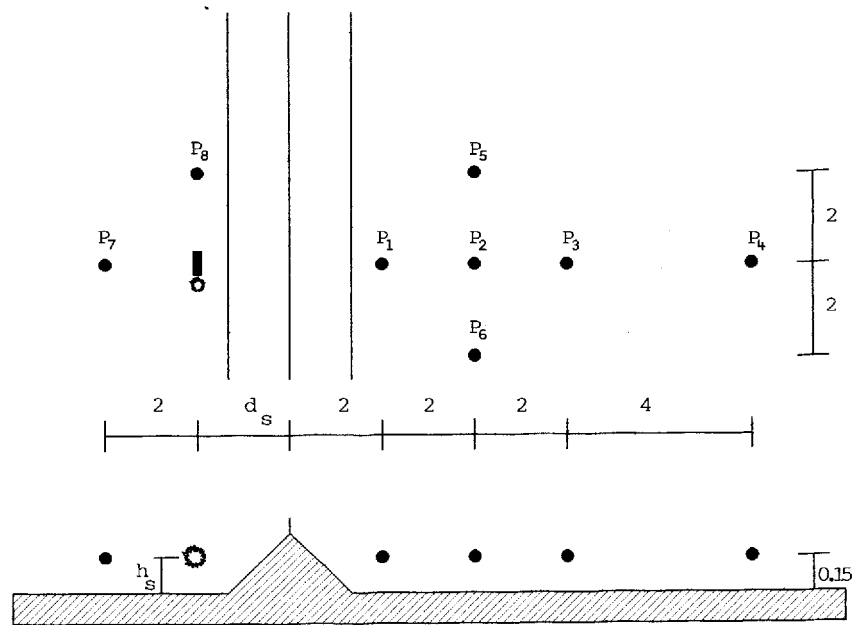

Figure 1   Experimental set-up 1:10 scale model tests. The points labelled P1 to P8 are pressure transducer locations; d_s and h_s indicate the location of the source (detonator). All dimensions are given in metres.

Two types of blast walls were investigated: a 0.5 m high screen and a 0.4 m high dike with a 0.1 m high screen on top. The latter barrier is a model of the one in use at the actual training site. To minimise acoustic absorption, the barriers were made of acoustically hard 10 mm thick plywood. The ground, concrete tiles, on the test site was levelled to minimise terrain effects.

The muzzle blast from a 155 mm howitzer was simulated with an electric detonator. To eliminate sideward expansion of the blast, the detonator was mounted inside a 10 cm long metal cylinder ($\varnothing$ 4 CM), leaving some space to simulate the barrel of a weapon. The overpressure levels in the blast generated by a l 55 mm howitzer varies from 100 kPa in the immediate surrounding of the weapon to about 4 kPa at 25 m, with a positive phase duration of the order of 6 ms. According to the Hopkinson scaling law, the positive phase duration of the blast wave in the scale model experiments should be reduced by the same amount as the length scale, yielding a duration of 0.6 ms. The selected detonator, a nr. 8 with a charge equivalent to 1.4 g TNT, gives a peak overpressure of 4.7 kPa and a phase duration of 0.6 ms at a distance of 2.5 m, which meets the requirements fairly well. However, the peak overpressure of the blast generated by the detonators is varies by about 10 %. In addition, the piezo-electric pressure transducers that were used suffered from inaccuracies at this low pressure range which could not be removed by calibration. Therefore it was decided to repeat the tests three times and to apply an averaging procedure.

Two series of measurements were conducted. In the first series the distance between detonator and wall was varied from 0.5 to 2 m, with the detonator placed at a constant height of 0.2 m. In the second series the height of the source was varied from 0.02, i.e. ground level, to 0.4 m, with the detonator placed at a distance of 0.75 m from the wall. Both series were conducted with and without blast wall. At the beginning of each day of the measurement campaign, the wall was first removed to check the free-field pressure decay. Meteorological data, like the ambient pressure, temperature, wind speed and humidity were also recorded. All experiments were conducted on days of similar weather to minimise the effect of meteorological variations.

2.3   Results

In the following, the shielding efficiency of the walls will be evaluated on the basis of the reduction of the peak overpressure and the attenuation in dB(lin,peak).

In Figure 2 some typical pressure histories are shown. The shock wave diffracted by the screen clearly exhibits three distinct peaks with interarrival times of about 0.2 ms. These peaks coalesce further downstream. This typical non-linear feature is the so-called waveform steepening effect, i.e. waveform portions with higher overpressures move faster than those with lower overpressures resulting in a steepening of the wave front. At the distance of transducer P4 the three waves have accumulated into a single peak. For the dike-shaped wall, only two distinct peaks are found in the pressure histories. This clearly illustrates the difference in the diffraction process around the screen and the dike. Further downstream, however, the characteristic features of the diffraction process disappear due to the waveform steepening effect. Hence, the wall geometry is hardly critical to the conditions in the far field.

Figure 2 Pressure-time signals measured with transducers P1 to P4 behind the screen (left) and the dike (right),for $d_s = 0.5$ m and $h_s = 0.2$ m.
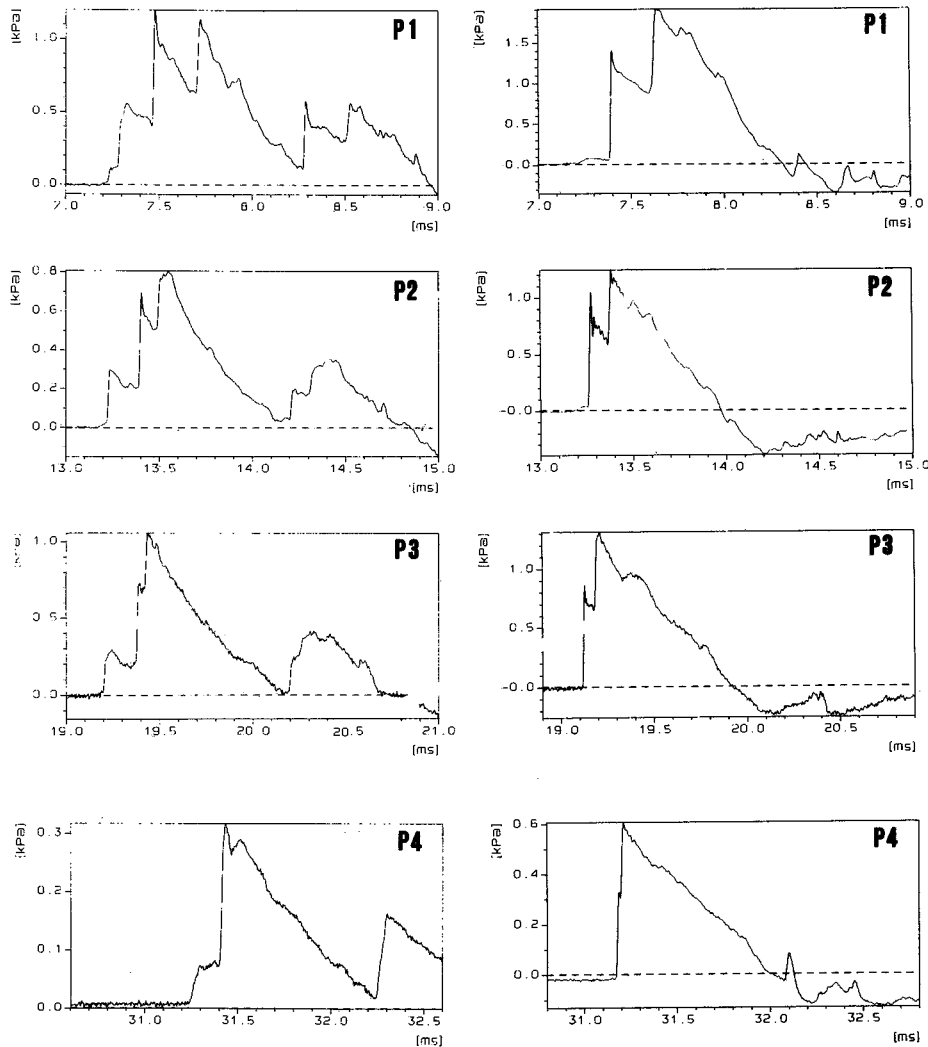

Figure 2   *Pressure-time signals measured with transducers P1 to P4 behind the screen (left) and the dike (right), for $d_s = 0.5$ m and $h_s = 0.2$ m.*

In Figure 3 and 4 the decay of the peak overpressure behind the screen and dike-shaped wall is shown for varying distance of the detonator to the wall. The corresponding values measured without the blast wall are also given in the graph. Figure 5 shows the attenuation by the screen and dike expressed in peak sound pressure level dB(lin, peak). From these figures it can be seen that close behind the screen the peak overpressure is reduced to about 30 % (10 dB reduction) of the unshielded overpressure, while further away the attenuation is about 50 % (5 dB reduction). Similar results are found for the dike-shaped wall, except that the attenuation

immediately behind the dike is less, about 40 % (8 dB).

The lower shielding efficiency found close to the dike is due to the fact that the diffracted wave will also contain a contribution from the upward reflected shock wave from the front of the dike and that there is lesser expansion space at the rear face, as compared to the screen. The fact that the shielding efficiency of a wall is maximal when it is placed as close to the source as possible is not clearly confirmed by our data, though this might be obscured by the relatively large experimental scatter of the results.

Figure 3 Measured peak overpressures behind the screen for varying distance of the detonator to the wall d_s (h_s = 0.2 m) and corresponding free field data.
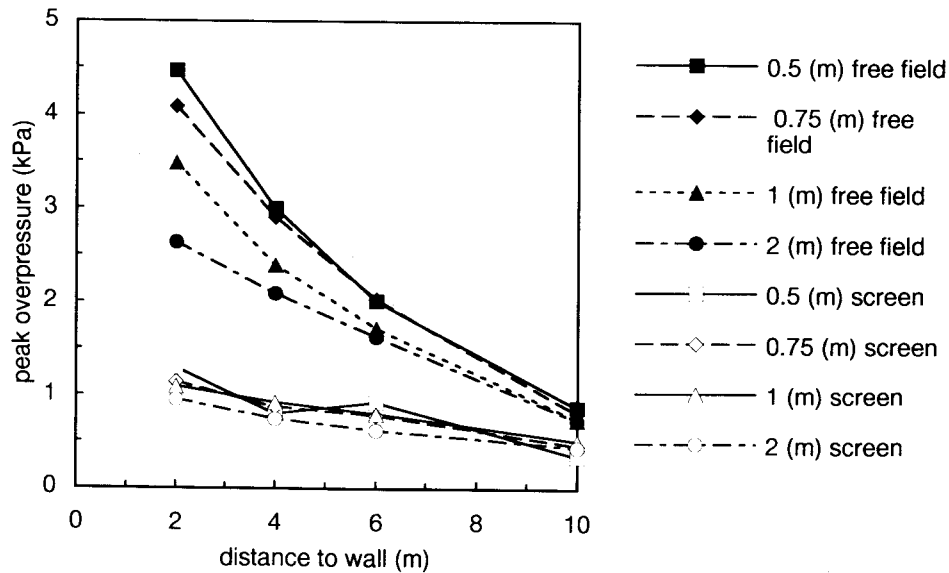

Figure 3   Measured peak overpressures behind the screen for varying distance of the detonator to the wall d_s (h_s = 0.2 m) and corresponding free field data.

Figure 4 Measured peak overpressures behind the dike for varying distance of the detonator to the wall d_s (h_s = 0.2 m) and corresponding free field data.

Figure 4   *Measured peak overpressures behind the dike for varying distance of the detonator to the wall d_S (h_S = 0.2 m) and corresponding free field data.*
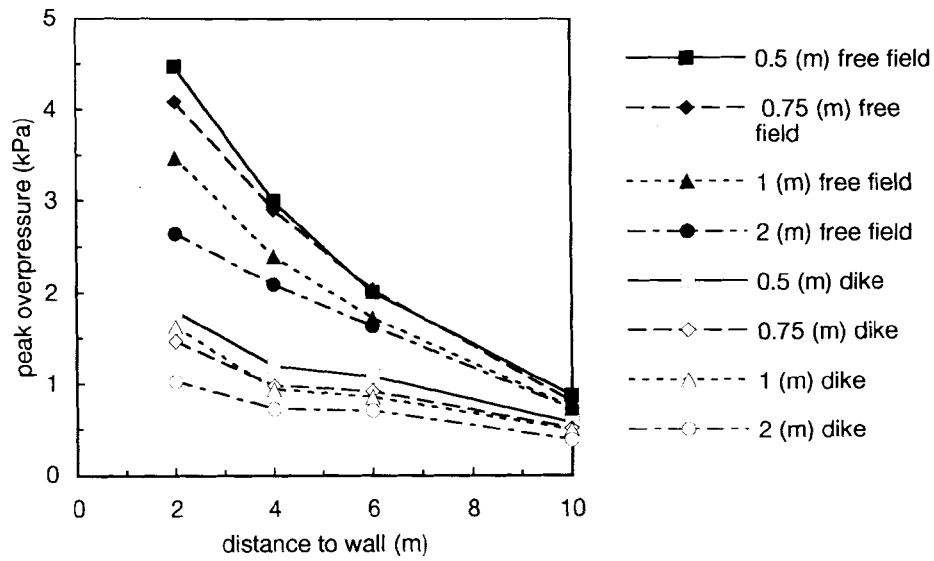
Figure 5 Peak sound pressure insertion loss for varying distance of the detonator to the wall d_s (h_s = 0.2 m).
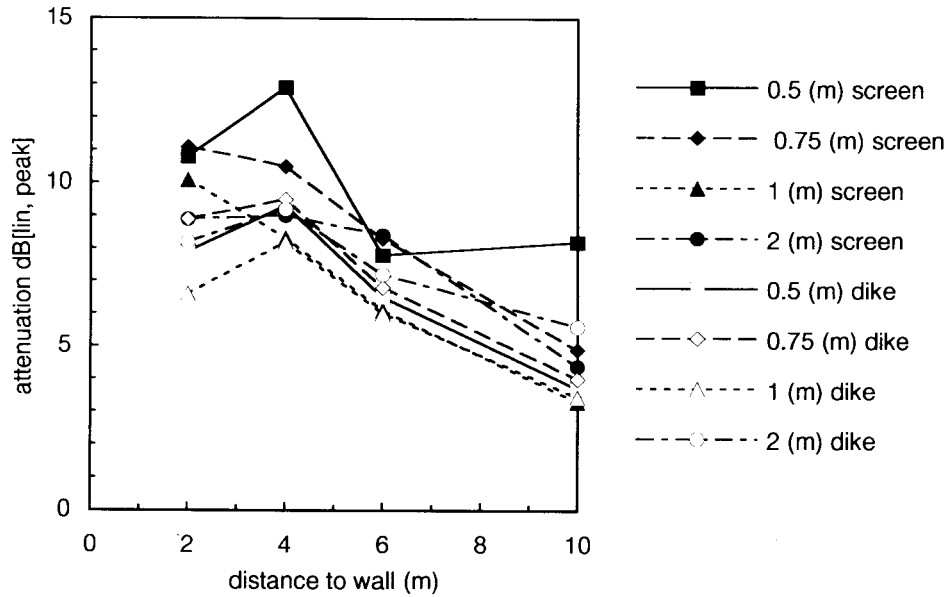

Figure 5   Peak sound pressure insertion loss for varying distance of the detonator to the wall d_S (h_S = 0.2 m).

The effect of the variation in height of the detonator on the shielding efficiency seems to be of the same order as the experimental scatter (l dB) such that it is impossible to draw any firm conclusions on the influence of the detonator height on the shielding efficiency.

2.4 Comparison with theory and calculations

At TNO-PML, a finite difference Computational Fluid Dynamics code called BLAST is used for the simulation of three-dimensional blast-object interaction. The BLAST code solves the Euler equations, which describe inviscid compressible flow. Flux-Corrected Transport is used to capture and preserve shock phenomena. Flux-Corrected Transport employs the qualities of both a first and a higher order finite difference scheme to obtain solutions with an optimum balance in accuracy and stability. As a consequence of its basic concept of inviscid flow, the BLAST code is expected to give accurate reproduction of the diffraction loading effects of blast. Viscous effects, which play a role in the drag loading of the structure, are not captured. However, overpressure and duration of the blast wave in combination with the dimensions of the object indicate that drag effects are of minor importance in the present study.

Some calculations were made with the two-dimensional version of BLAST and with the linear acoustic sound diffraction model TOMAS. Over the entire range, TOMAS generally predicted a 10 dB higher attenuation by the walls than measured. This large deviation is probably due to the fact that the shock waves produced by the muzzle blast are still too strong for the acoustic theory to be valid, since good agreement was found between the experimental data and

predictions by BLAST-2D.

3   Blast interaction with multiple obstacles

3.1   Purpose

Another research programme on blast diffraction over obstacles which we performed had a different purpose. The question to be answered by this study was to what degree rows of buildings at the edge of a city shield buildings that lay behind them from a blast wave which enters the city. Risk analyses for industrial complexes or ammunition storage sites are based upon undisturbed free-field pressures. If the overpressure level is significantly reduced due to the interaction with the first rows of buildings, this would lead to a large reduction in the amount of damage in the low overpressure region. The programme was focused on relatively low strength blast waves (l to 10 kPa) with durations comparable with a large vapour cloud explosion: about 60 to 100 ms.

3.2   Test set-up

The measurements were performed in the 40 x 40 cm^2 shock tube at TNO-PML. Two-dimensional rectangular blocks were used to simulate the buildings. The blocks (5 x 5 cm^2 cross section) were mounted across the test section of the shock tube. The test set-up was instrumented with pressure transducers, which were positioned centrally in the blocks.

Pressure information was also obtained from interferograms. The density field in the test section can be recorded by a shearing interferometer through windows in the shock tube. The interferograms record the density gradient and by doing so, they give a visualisation of the positions of the shock waves as well. The light fringes in the interference pattern indicate lines of constant density gradient. By counting the light fringes from a position where the pressure is known one can obtain the pressure in the entire flow field.

The size of urban housing and the mutual distance between houses in a city is typically of the order of 10 metres. Hence, in the experiments the geometry was scaled by a factor of 200. According to the Hopkinson scaling law the characteristic times should be scaled with the same factor as the length scale. Hence, the positive phase duration of the blast wave in the scale model experiments should be reduced to 0.5 ms. By reducing the length of the driver section to about 5 cm a positive phase duration of about 1.5 ms could be realised, which did not completely meet the requirements. The BLAST code was used in conjuction to the shock tube experiments to simulate the blast interaction. The two-dimensional version of the BLAST code, called BLAST-2D, was used to simulate this flow in a rectangular grid consisting of 350x200 cells.

3.3   Results

The first configuration investigated concerned a blast wave of 10 kPa overpressure and 60 ms duration falling in at two 10 m high buildings located IS m behind one another. In Figure 6

both the measured interferograms as well as the pressure field calculated from the numerical simulation are shown. The calculated pressure distribution is visualised by an isobar pattern, showing one isobar for each pressure increase of 0.5 kPa. The first interferogram shows the vertical shock wave striking the structure from the left. The strong discontinuity at the shock front causes light refraction producing the dark line on the image. In the numerical simulation, due to the discontinuous pressure jump over the shock wave, the isobars are accumulated also resulting in a dark line at the position of the shock wave.

After the shock strikes the first structure, part of the shock wave is reflected backwards, as shown in the second picture. The overpressure in the reflected shock is about a factor of two greater than that of the incident shock. The pressure difference causes a flow from the region of high to low pressure, resulting in the formation of circular expansion waves at the corners of the structure. Since these expansion waves exhibit only minor pressure variations, they cause little light refraction and are visible as minor distortions of the interference pattern, i.e. individual fringes can be identified. The numerical simulation shows distinct isobars in this region, similar to the fringes in the interferogram. At the edge of the structure, viscous separation occurs generating a rolled-up vortex featuring a steep density gradient. Hence, the fringes are accumulated at the vortex, producing a dark spot. In the third picture, the shock wave has passed the rear face of the first structure, showing expansion waves that bridge the pressure difference between the induced air flow above the buildings and the undisturbed flow in between. The expansion waves travel downward across the rear face of the first building. At the edge of the rear face, a second vortex is formed.

The fourth picture shows the complicated wave pattern that develops in-between the two buildings. The front of the second building will be hit by the diffracted wave originating from the rear edge of the first building. Obviously, the blast loading on the second building will be significantly influenced by the presence of the first building, as expected. Next, the infalling wave on the second building is reflected back, which is attended by an increase in overpressure, and the rear face of the first building is hit again, as shown in the last picture. This explains why the rear face of a building also shows significant damage after an accidental explosion when it is closely surrounded by other buildings.

All pictures shown in Figure 6 represent the diffraction phase of the shock wave loading on the structures. After passage of the shock wave, the pressure discontinuities travel outwards and the load imposed on the buildings is mainly due to aerodynamic drag produced by the air flow, which is referred to as drag-phase loading. Taken along by the air flow, the vortices have expanded and are propagated further away from the corners.

Figure 6 Experimentally obtained interferograms (left) and the pressure fie Id as obtained from numerical simulation (right),for a blast wave of 10 kPa and 60 ms duration.
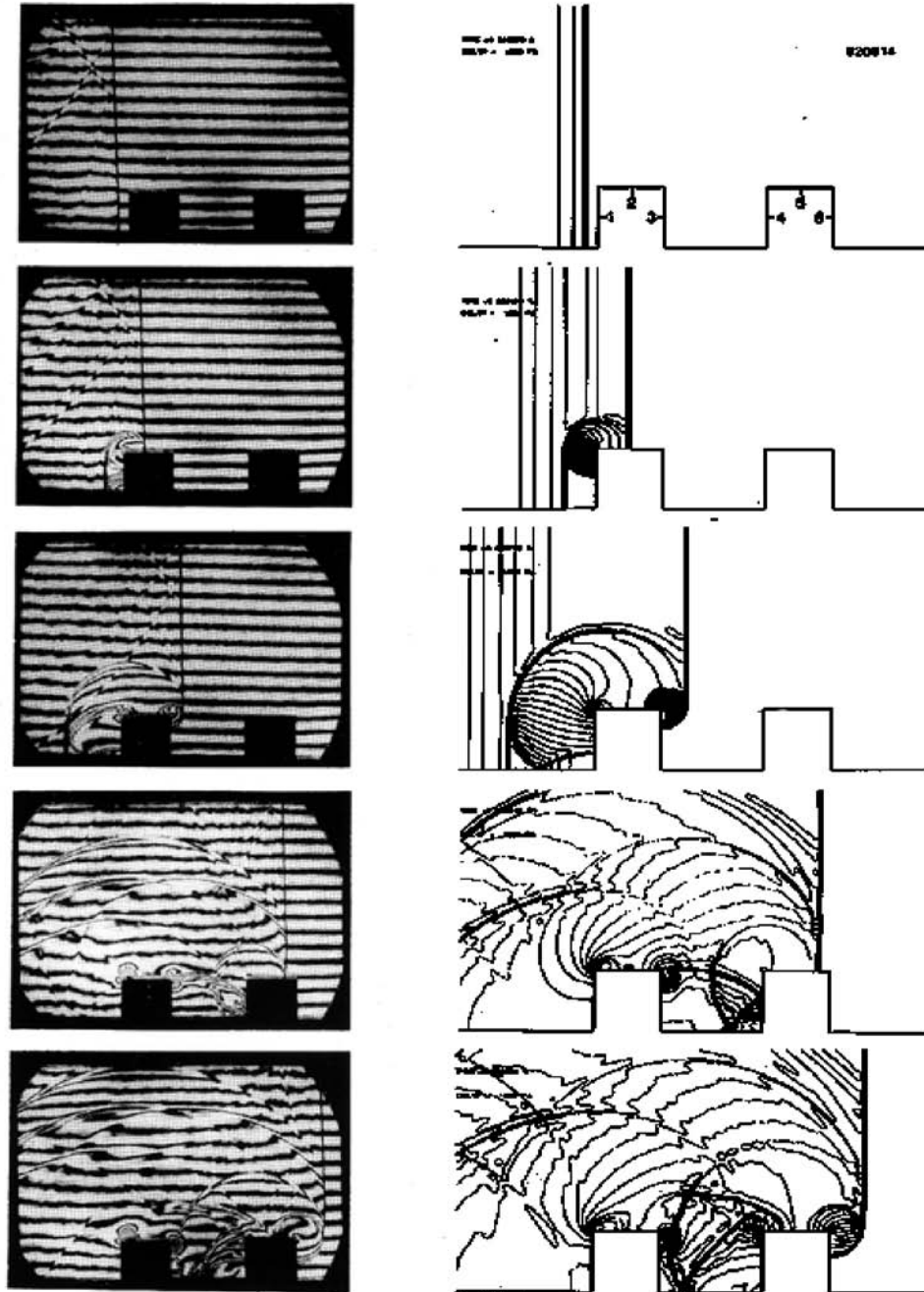
Figure 6   Experimentally obtained interferograms (left) and the pressure field as obtained from numerical simulation (right), for a blast wave of 10 kPa and 60 ms duration.

The overpressure histories as calculated with BLAST-2D at the front, the top and the back of the two buildings are shown in Figure 7. In these overpressure signals the complicated wave pattern can be readily recognised. The overpressure signal predicted at location 3, at the back of the first building, for instance shows a sequence of four shock phenomena which can be traced in the flow patterns shown in Figure 6. The first corresponds with the passage of the shock of the infalling blast wave. The gradual pressure build-up is the result of the diffraction of the shock around the first building. The second pressure jump corresponds with the reflection of the primary wave by the ground. The third pressure increase corresponds with the infalling shock wave reflected directly from the second building. This shock wave is immediately followed by a fourth wave, which is a result of the reflection by the second building and subsequently by the ground. Because the second structure is hit by the expansion wave originating from the rear edge of the first building, the blast load on the front of the second building will be lower than the load on the front of the first structure. The computation shows that the blast overpressure experienced by the front of the second building is about 2.5 times lower than the reflected overpressure of the undisturbed blast wave endured by the front of the first building. Further investigations showed that this reduction depends also on the positive phase duration. Investigations with more than two obstacles also revealed that the pressure did not reduce significantly when more obstacles were used.

Figure 7 Pressure-time signals at positions 1 to 6 (see Figure 6) as calculated for the blast wave of 10 kPa and 60 ms duration interacting with two 10 m high buildings.

Figure 7   *Pressure-time signals at positions 1 to 6 (see Figure 6) as calculated for the blast wave of 10 kPa and 60 ms duration interacting with two 10 m high buildings.*
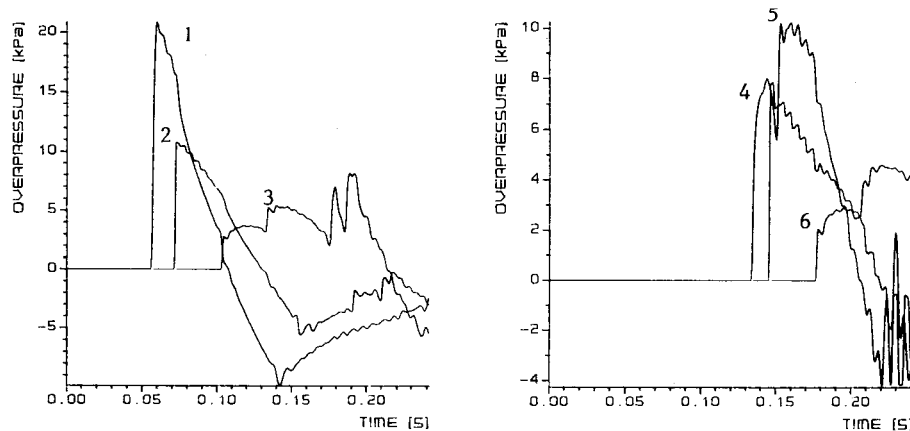
3.4   Comparison between shock tube results and BLAST simulation

To enable a comparison between measured and calculated signals, a computation was conducted for a test environment that could actually be realised in the shock tube, i.e. a blast wave of 7.5 kPa peak overpressure with a positive phase duration of 1.5 ms falling in at two 5

cm high structures standing 7.5 cm apart. Figure 8 shows a comparison between the pressure histories measured and calculated at the front and the rear face of the first structure, and at the front of the second structure. Very striking is the good resemblance of the two series of signals. Both series show nearly the same reflections. In-between the two obstacles, the simulation predicts somewhat higher overpressures.

Figure 8 Comparison between measured pressure histories and calculated signals at positions 1, 3 and 4 for a blast wave (7.5 kPa, 1.5 ms)falling in at two structures (5 cm high)

Figure 8   *Comparison between measured pressure histories and calculated signals at positions 1, 3 and 4 for a blast wave (7.5 kPa, 1.5 ms) falling in at two structures (5 cm high)*
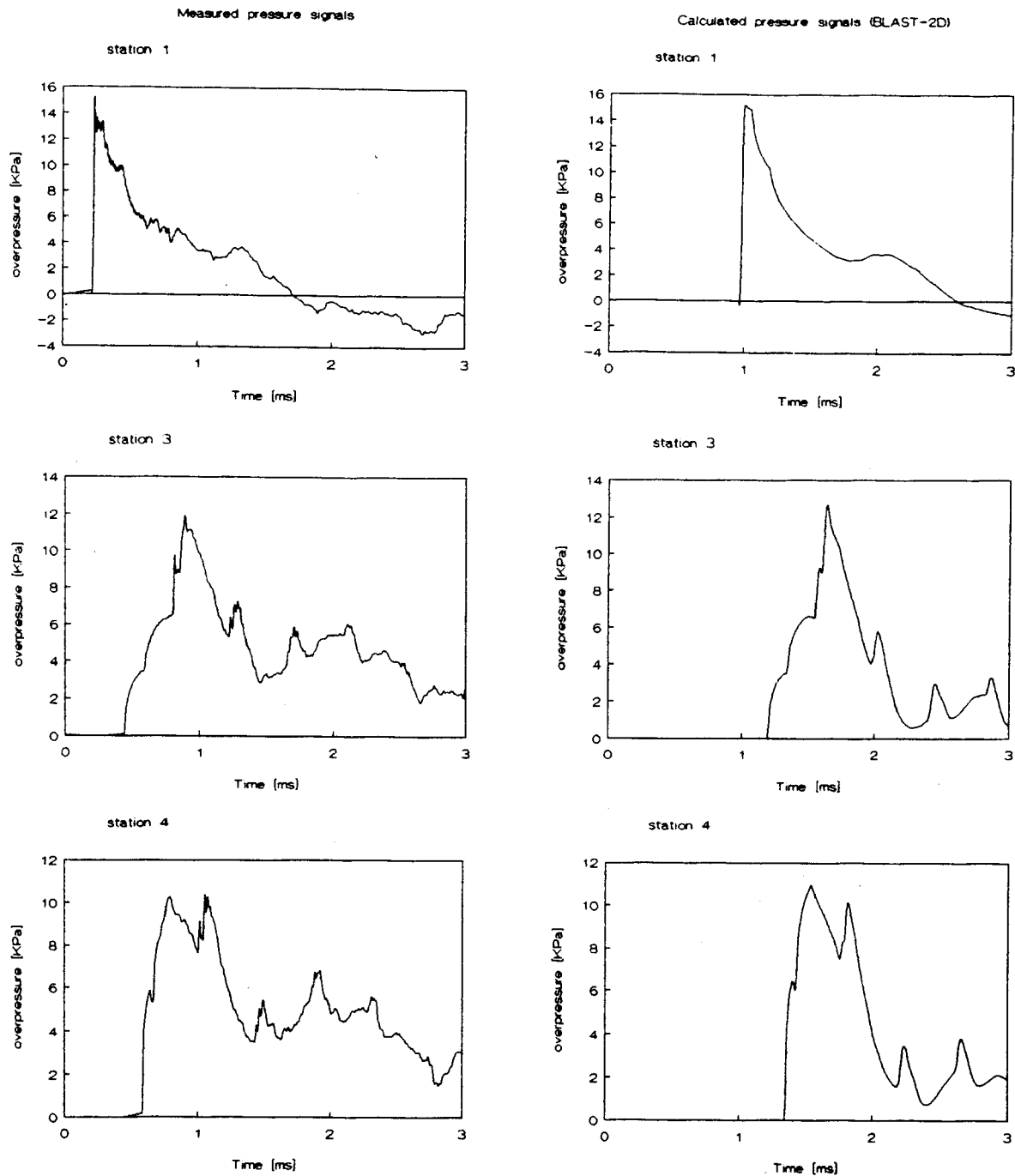
4 Pressure development in a chamber due to an entering shock wave

4.1 Purpose

For the determination of structural damage due to a shock wave, the pressure distribution on the structure and structural elements, has to be known. Most of the existing models consider the structure as fully closed. The observed damages in full scale tests have shown the importance of the delayed pressure build-up through window and door openings for the damage level and damage mechanisms: sometimes the buildings appeared to be burst open due to internal pressure rather than being crushed in due to the overpressure in the shock wave.

At the request of the Co-ordinator Civil Emergency Planning of the Ministry for Housing, Physical Planning and Environment, an experimental programme was performed at TNO-PML. The aim of the programme was to study the pressure development inside a chamber when a shock wave enters through a window and gather experimental data to describe the load on the walls with empirical expressions.

4.2 Test set-up

The shock wave was generated with a blast simulator with a 2 m diameter end section. This size limited the maximal dimensions of the window. The volume of the chamber was chosen to obtain an area ratio of the window and the internal walls in the range of 2 to 5 %. This variation will be present in normal buildings. The chamber was made out of a standard 10 ft transport container, which was cladded internally with steel plates to create smooth walls. A hollow steel frame with removable panels for the creating of different sized windows was placed between the container and the exit of the blast simulator. The internal dimensions of the chamber were 2.92 x 2.33 x 2.37 m^3. The chamber could be halved in length by placing a panel in the container.

The incident shock wave, the pressure distributions on the front wall and inside the chamber were recorded with piezo-resistive pressure transducers. The signals were digitally recorded and were numerically processed afterwards. Figure 9 gives a schematised horizontal cross section and the transducer locations. More information is given by Weerheijm and Mercx [1991] and Mercx [1990a, 1990b, 1991].

A total of 133 shots were fired in the test programme. The incident peak overpressure was varied between 2 and 8 kPa, six window sizes between 0.42 x 0.42 m^2 and 1.2 x 1.2 m^2 were used, the chamber depth was varied between full depth and half depth, and the window was either left open or closed with a glass pane of various strength.

4.3   Description of results

When the generated shock wave reaches the front face of the container, a complex process of reflection, rarefaction and expansion starts. Figure 10 gives schematised drawings of the waves at successive points of time, while in Figure l1 the pressure histories for the test with a 1.2 x 1.2 m^2 opening and the full length chamber are given. When the process is followed in time, we see first the pressure on the outside of the front wall doubled by reflection (location Dl). This pressure decreases rapidly due to the initiated rarefaction wave at the edges of the oriflce. At the same time the shock wave expands into the chamber and loads the front wall from the inside (location D2). The expanding wave reflects against the side walls of the chamber (locations D4, DS and D6). A shock front is formed by the initial wave and these reflections, which runs through the chamber and hits the rear wall (location D7). The duration of the shock front is reduced to some milliseconds by the internal rarefaction process, see Figure 10.

After the passage of the initial shock and its reflections a relatively slow pressure build-up takes place within a certain rise time, tr. This pressure build-up is almost identical for all the walls. After the pressure reaches its maximum it decays again in a vent time, tv, after which a negative phase occurs, see Figure 12.

The pressure development appeared to be composed of two phases, i.e. the initial process of travelling and interacting shock waves which is followed by a process of a relatively slow pressure rise and subsequent venting.

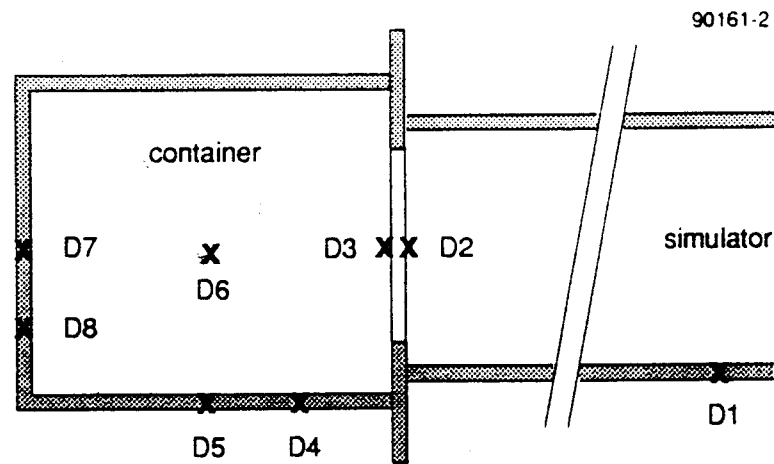# Figure 9 Schematic horizontal section of the chamber showing the position of the pressure transducers

90161-2

container

D7   **x**   D3 **x x** D2   simulator

D6

D8

D5   D4

D1

Figure 9   Schematic horizontal section of the chamber showing the position of the pressure
                  transducers

Figure 10 Position of shock waves at successive points of time using linear acoustic theory
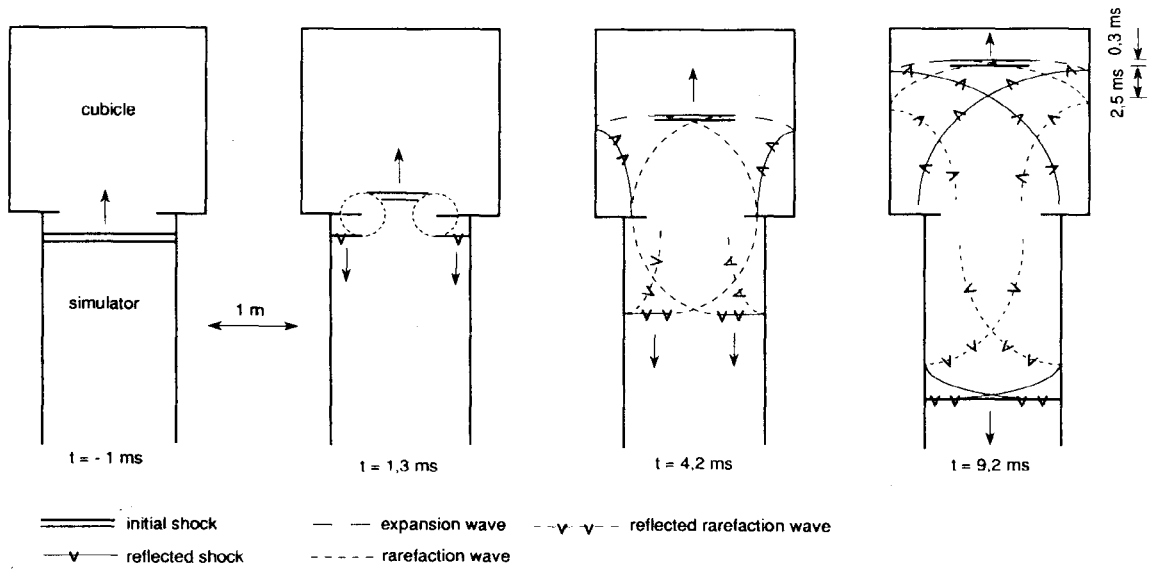

Figure 10   Position of shock waves at successive points of time, using linear acoustic theory

**Figure 11 Pressure recordings in the blastsimulator and chamber at the
locations D1, D2, D3, D4, D5, D6 andD7. This test was with a 1.2 x 1.2 m²
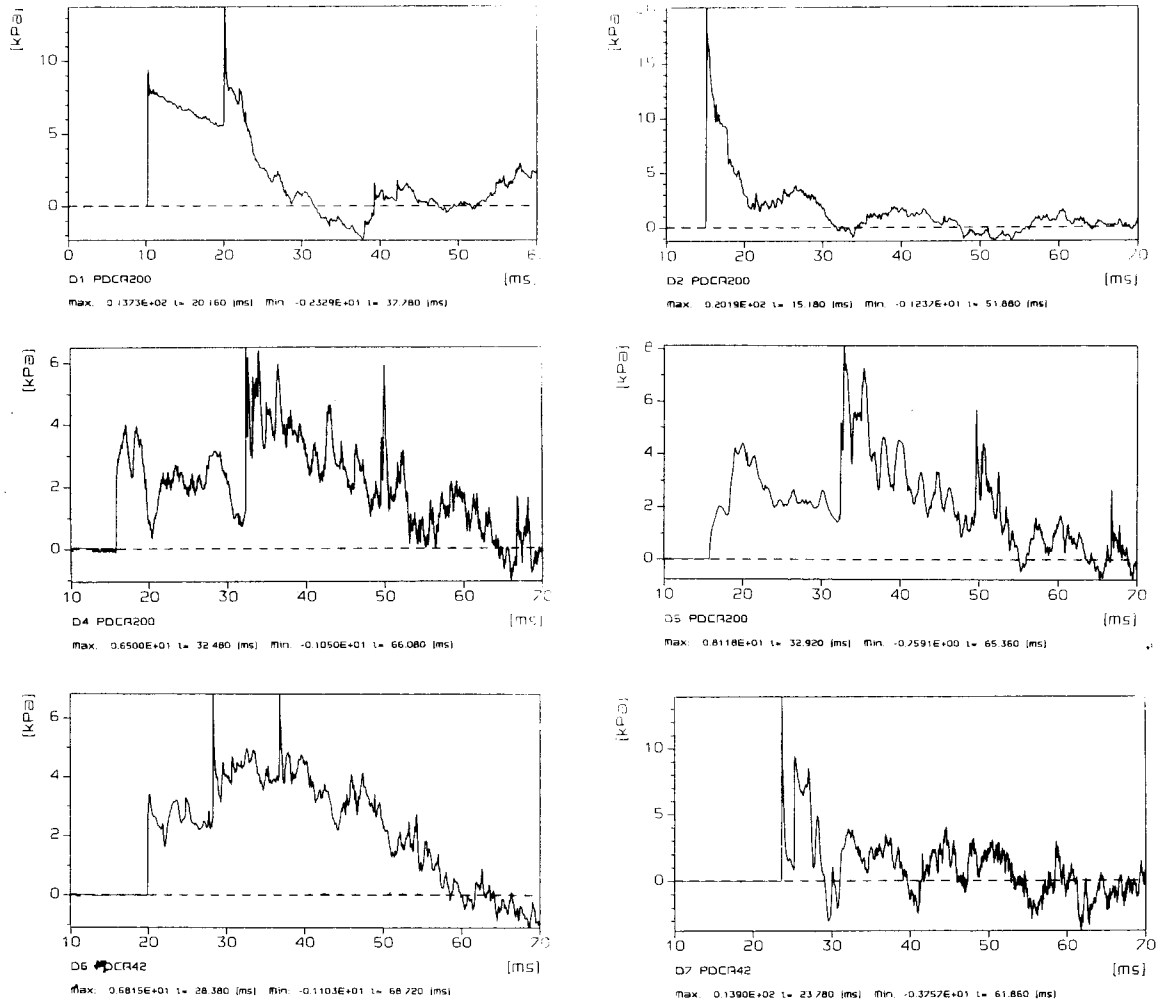opening and the full length chamber**

*Figure 11   Pressure recordings in the blastsimulator and chamber at the locations D1, D2, D3, D4,
D5, D6 and D7. This test was with a 1.2 x 1.2 m² opening and the full length chamber*

4.4   Influence of chamber depth

In view of the described processes it will be clear that chamber depth related to the length of
the incident shock wave must be an important parameter for the pressure development process
inside structures. It appeared from the test results that the chamber depth had no qualitative
influence on the wave phenomena, only the time scale of the passing reflection waves was
affected. The reduced chamber depth had more influence on the slow pressure build-up after
the first phase: it caused the overall pressure to increase. It emerged that the overall pressure

can even be higher than the overpressure of the incident shock wave. The opposite is true for the venting time, which decreased considerably. The smaller chamber dimensions enabled a quicker response to the pressure outside the chamber. It was possible to derive empirical relationships for the pressure on the internal walls [Mercx, 1991] which are compatible with the existing relations for the load on the external walls [Glasstone, 1957].

4.5   Influence of glass panes

The influence of the window panes was remarkable. The window panes failed very quickly (less than 10 ms) but the fragments formed a dense screen and a major part of the incident shock was reflected. The reflected shock was comparable to the shock reflected from a rigid wall. There are no rarefaction waves visible in contrast to the case without the window pane.

The influence on the internal pressure is even greater. The shock waves are completely eliminated, the pressure rise is rather smooth while the positive phase duration is slightly shorter. The maximum pressure was reduced to 25 %. During the negative phase the window is completely open and the pressures are comparable for both types of tests. It should be noted that when the positive phase of the shock wave is long compared to the time for the window to fail and the fragments to disperse, the observed reduction of the internal pressure might be significantly smaller. Generalising the results it can be stated that the presence of windows reduced the maximum internal pressure about 15 to 40 % while the positive impulse was reduced to 20 %.

Figure 12
The internal pressure at the side wall without a) and with b) a window pane
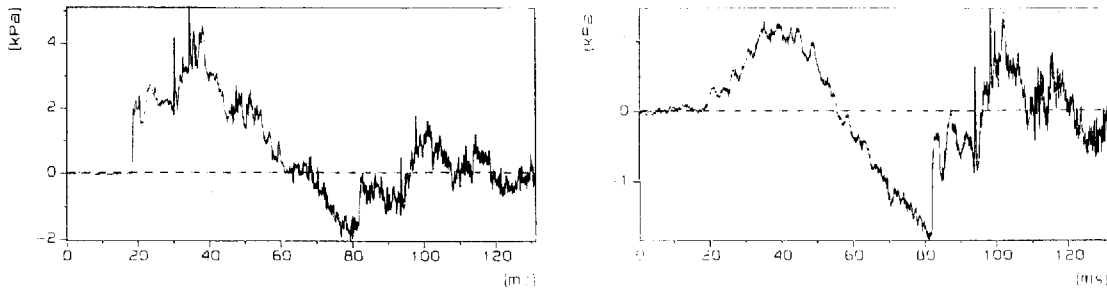

Figure 12   The internal pressure at the side wall without a) and with b) a window pane

5   Conclusions

These three research programmes again showed that the interaction of shock waves with structures is strongly dependent on the geometry of the structure and also depends on the overpressure and phase duration of the shock wave. They also showed that shielding of a shock wave by blastwalls or buildings can result in significant reductions in shock strength. The most surprising result was that a shock wave can reflect almost entirely on a pane of window glass, even during the phase when the pane is already broken and the fragments are hanging in the air.

As far as prediction methods are concerned, the programmes showed that linear acoustic prediction methods can in some cases, like diffraction, give good predictions, but fail when non-linear effects become important. This is the case for example with reflection and wave steepening. Therefore this method should not be used for shocks stronger than about 1 kPa, or be used only as a first approximation. The numerical predictions with the Computational Fluid Dynamics code BLAST proved to be reliable.

6   References

Absil, L.H.J.; A.C. van den Berg and J. Weerheijm Blast interaction with multiple obstacles Proceedings MABS 13, Den Haag, 1993.

Absil, L.H.J.; H.H. Kodde and W.P.M. Mercx The effectiveness of blast walls Proceedings MABS 13, Den Haag, 1993.

Bakkum E.A.
The effectiveness of blast walls in reducing sound levels of large-caliber weapons (in Dutch)
TNO Prins Maurits Laboratory, PML 1990-71, Rijswijk, 1990.

Bakkum E.A.; J. Weerheijm and H.J. Pasman Diffraction of weak shock waves by barriers
Proceedings MABS 12, Perpignan, 1991

Glasstone, S.
The effects of nuclear weapons
US Atomic Energy Commission, Washington, 1957.

Mercx, W.P.M.
Pressure development in a chamber due to an entering shock wave
TNO Prins Maurits Laboratory, PML 1990-C1, Rijswijk, 1990.

Mercx, W.P.M.
Pressure development in a chamber due to an entering shock wave Part two: influence of window panes
TNO Prins Maurits Laboratory, PML 1990-C122, Rijswijk, 1990.

Mercx, W.P.M.
Pressure development in a chamber due to an entering shock wave Part three: Variation of chamber depth and final results TNO Prins Maurits Laboratory, PML 1991-C34, Rijswijk, 1991.

Weerheijm, J. and W.P.M. Mercx
Pressure development in a chamber due to an entering shock wave
Proceedings MABS 12, Perpignan, 1991.